



Review

A Review on the Application of 3D Printing Technology in Pavement Maintenance

Fangyuan Gong ^{1,*}, Xuejiao Cheng ¹, Qinghua Wang ², Yi Chen ³, Zhanping You ⁴ and Yu Liu ⁵

¹ School of Civil and Transportation Engineering, Hebei University of Technology, 5340 Xiping Road, Beichen District, Tianjin 300401, China

² Shandong Provincial Communications Planning and Design Institute Group Co., Ltd., Tianchen Road 2177, Jinan 250101, China

³ Road and Bridge School, Zhejiang Institute of Communications, No. 1515, Moganshan Road, Hangzhou 311112, China

⁴ Department Civil, Environmental, and Geospatial Engineering, Michigan Technological University, 1400 Townsend Drive, Houghton, MI 49931, USA

⁵ School of Highway, Chang'an University, South Erhuan Middle Section, Xi'an 710064, China

* Correspondence: fgong1@mtu.edu or fgong1@hebut.edu.cn

Abstract: To examine the application and significance of 3D printing technology in pavement maintenance engineering, a review of the current developments in principles, types, materials, and equipment for 3D printing was conducted. A comparison and analysis of traditional methods and 3D printing for asphalt pavement maintenance led to an investigation of 3D asphalt printing technologies and equipment. As a result, the following suggestions and conclusions are proposed: 3D printing technology can increase the level of automation and standardization of pavement maintenance engineering, leading to effective improvements in worker safety, climate adaptability, repair accuracy, etc. For on-site repair of cracks and minor potholes, utilizing material extrusion technology a mobile 3D asphalt printing robot with a screw extrusion device can be used for accuracy and flexibility. For efficient repair of varying cracks, material jetting technology with a UAV equipped with a 3D printing air-feeding device can be employed.



Citation: Gong, F.; Cheng, X.; Wang, Q.; Chen, Y.; You, Z.; Liu, Y. A Review on the Application of 3D Printing Technology in Pavement Maintenance. *Sustainability* **2023**, *15*, 6237. <https://doi.org/10.3390/su15076237>

Academic Editors: Mohammad Reza Khosravani and Payam Soltani

Received: 20 February 2023

Revised: 29 March 2023

Accepted: 3 April 2023

Published: 5 April 2023



Copyright: © 2023 by the authors. Licensee MDPI, Basel, Switzerland. This article is an open access article distributed under the terms and conditions of the Creative Commons Attribution (CC BY) license (<https://creativecommons.org/licenses/by/4.0/>).

1. Introduction

Prolonged traffic loads and environmental factors can cause asphalt pavement [1–3] to develop cracks, potholes, and other forms of distress [4–6]. If not addressed promptly, these distresses can escalate and compromise the road structure and traffic safety. With a vast road network and a high proportion of maintenance required, maintaining roads in China is a very challenging task [7]. The most common methods for repairing cracks in asphalt pavement are pouring, sealing, and digging-patching, using materials such as modified asphalt and resin [8,9]. For pothole repair, traditional methods involve removing old material and filling with new material, using either hot-mixed or cold-mixed asphalt mixture [10]. These maintenance methods often require multiple workers and can be time-consuming and risky, especially in areas with heavy traffic [11]. They also rely heavily on manual labor, reducing the ability to withstand changing weather and environmental conditions [12]. Additionally, individual differences among workers can lead to a lack of precision and standardization in maintenance engineering.

As an important method under the umbrella of additive manufacturing, 3D printing technology combines cutting-edge technologies such as 3D digital modeling, electromechanical control, computer science, material science, and structural mechanics [13]. Further, 4D printed parts that can alter their shape over time because of their dynamic capability are also gradually developing [14]. As a crucial part of the “third industrial revolution”,

3D printing technology has found applications in fields such as biomedicine, industrial manufacturing, food processing, aerospace, and civil engineering [15,16]. With its advantages of automation, high efficiency, and precise control, 3D printing is increasingly being used in road engineering. In 2018, Jaeheum et al. [17] created a 3D digital model of concrete pavement potholes using multi-dimensional photography and photogrammetric software algorithms. When a 3D-printed plastic mold corresponding to the damaged areas is used to cast concrete patches, the time spent blocking the road could be reduced from 7 d to 2 h, resulting in economic benefits. By leveraging the automation, efficiency, and precision of 3D printing technology in pavement maintenance, the risks, inefficiencies, and quality issues associated with manual labor can be reduced. However, there remains a need for more comprehensive discussion and analysis on the subject.

The objectives of this paper are as follows: (1) summarize the advancements in 3D printing technology, covering its underlying principles, techniques, materials, and equipment. (2) Assess the benefits of using 3D printing technology for fixing pavement problems such as cracks and potholes, based on an investigation of these issues and traditional repair methods. (3) Conduct an in-depth analysis of the feasibility and options for integrating 3D printing technology into pavement maintenance projects from various perspectives such as material, type, and equipment. (4) Offer insights on the future direction of 3D printing technology in pavement maintenance engineering.

2. Development of 3D Printing Technology

2.1. Principle of 3D Printing Technology

To be sure, 3D printing is a primary implementation form of additive manufacturing. Various terms such as solid freeform fabrication (SFF), rapid manufacturing (RM), and additional layer manufacturing (ALM) have been used to define this technology. Unlike subtractive manufacturing [18], which involves cutting, carving, and grinding of raw materials, 3D printing is an additive manufacturing technology that creates objects by building them layer by layer using various materials, such as fluids, powders, filaments, and plates. The basic principle of 3D printing is discrete/accumulation [19]: (1) discrete refers to slicing the 3D digital model of the object using an algorithm; (2) accumulation refers to building the object layer by layer in the direction of the build, based on the sliced digital model.

2.2. Type and Material of 3D Printing Technology

According to ISO/ASTM 52900–2021 [20], there are more than 50 different types of additive manufacturing technologies, which are grouped into seven main categories: vat photopolymerization, material jetting, directional energy deposition, power bed fusion, sheet lamination, binder jetting, and material extrusion.

Vat photopolymerization [21] is one of the earliest forms of 3D printing and is considered to be a well-established technology. It can be further divided into three subtypes based on the photopolymerization characteristics of photosensitive resin materials: stereolithography (SLA), digital light processing (DLP), and PolyJet [22,23]. (1) SLA [24] technology uses ultraviolet (UV) light to scan the liquid photosensitive resin in successive dots along the cross-section profile of each layer after slicing the component model with computer assistance. The components are built layer by layer along the liquid surface with the moving down of the printing platform. (2) DLP technology [25] is similar to SLA, and its printing speed is faster with the utilization of a high-resolution digital light processor. One section of the object could be built with the projection of UV light. (3) PolyJet technology [22] is one type of material jetting technology, and the component is molded with cured photosensitive resin droplets by UV light. Compared with the fusing, binding, and extruding processes of other 3D printing technologies, the vat photopolymerization is a microscopic molding process with the advantages of high accuracy and a fine surface. However, because this kind of technology is applicable only to photosensitive resin materials, the types of materials are limited.

Common materials such as polymer [26] and metal [27] are fused by energy beams (lasers, electron beams, and plasma arcs) in directional energy deposition [28–30] and powder bed fusion technologies [31,32] to build structures. The main difference between these two technologies is that directional energy deposition technology [33,34] constructs the target object through delivering the materials to the molten pool generated by an energy beam, while powder bed fusion technology uses energy beams to fuse the selective powder bed according to the slice of the component digital model to complete the 3D printing process. So, the directional energy deposition technology has the characteristics of unlimited forming space, and the powder bed fusion technology has relatively high strength and resolution.

In the case of sheet lamination technology, objects are constructed by stacking sheets (such as paperboard, metal plates, plastic plates, etc.) that have been cut by laser or other energy beams, without the need for a support structure. The cutting process of sheet lamination technology usually results in a large amount of material waste and low printing accuracy. Additionally, binder jetting [35] and powder bed fusion [36] are the other two typical 3D printing technologies without a support structure. During the printing processes of these two technologies, the object is supported by the surrounding powder, and the excess powder can be recycled after printing. Directly printed components using binder jetting technology typically require post-processing to attain sufficient strength. Meanwhile, rough surfaces from directional energy deposition, powder bed fusion, and sheet lamination require grinding and polishing processes to improve their finish.

For material extrusion [37,38] technology, plastic materials are extruded in filamentary form onto a printing platform and solidified layer by layer to form components. This technology is low cost, and many materials can be selected, including acrylonitrile-butadiene-styrene (ABS) [39], polylactic acid (PLA) [40], thermoplastic polyurethane (TPU) [41], PLA-TPU [42], nylon [43] and other thermoplastic materials. ABS prints smoothly, has a pungent smell and high shrinkage in cold environments. PLA is printed almost without shrinkage and the pungent smell, but the extrusion head is easily blocked due to its good adhesion and ductility. In addition, great achievements of extrusion technology have been made in the 3D printing fields of cement mortars [44], liquid metals [45], ceramics [46], drugs [47], and biological material. However, the issue of material layer anisotropy in the 3D printing process using material extrusion technology has not been fully addressed. The connection between printing parameters such as layer thickness, printing speed, feed rate, temperature, and nozzle size and shape and their impact on the printing outcome remains unclear.

Table 1 displays the type, printing principle, and typical materials of the seven main types of 3D printing technology.

Table 1. Comprehensive evaluation of 3D printing technology [20–52].

Type	Printing Principle	Typical Materials
Vat photopolymerization	With the decline of the printing platform, the photosensitive resin is scanned layer by layer along the liquid surface using UV with a specific wavelength and intensity.	Photosensitive resin
Material jetting	Structures are formed on the printing platform layer by layer with the deposition of photosensitive resin droplet or nano-particle jetting (NJP).	Photosensitive resin, metal powders, ceramic powders, cement mortars, etc.
Directional energy deposition	Materials are delivered to the melt pool created by energy beams such as lasers, electron beams, and plasma arcs. Then the materials are melted and deposited layer by layer to form structures.	Metal powders, metal wires, plastics, etc.

Table 1. Cont.

Type	Printing Principle	Typical Materials
Power bed fusion	The structures are formed layer by layer through the process of repeated powder laying and selective sintering of the powder on the printing platform with energy beams such as laser beams and electron beams.	Polymer, metal powders, etc.
Sheet lamination	Tools such as lasers are used to cut layers of sheets to form 3D entities. The layers are usually joined by binders or bolts or by welding.	Paper board, plastic and metal sheets, etc.
Binder jetting	Dosed powder is tiled by the roller tiles on the printing platform and is bonded by the selective glue to build the component layer by layer.	Metal, ceramic, metal–ceramic composite powders, etc.
Material extrusion	Thermoplastic materials are extruded on the printing platform in the form of long filaments after melting and deposited layer by layer to form structures.	Thermoplastic, cement mortar, liquid metal, ceramic, pharmaceutical, bio materials, etc.

2.3. Equipment of 3D Printing Technology

The most commonly used 3D printing equipment can be classified into three main categories based on their movement system, as shown in Table 2: gantry, robotic arm, and cable robots [53]. (1) A gantry robot is also called a Cartesian or linear robot, and its advantages are simple calculations, intuitive expression in space, higher accuracy, and wide use. It is equipped with servo motors in the X, Y, and Z axes, respectively, and any position in the three-axis space area could be accurately located by linear movement on the X, Y, and Z axes. The printing scale is determined by the movement ranges of three axes, and large-scale gantry robots could be applied to an architectural-scale project. (2) The transmission method of the robotic arm swing between the big and small arm of the robot is similar to the movement of the elbow and shoulder joints in the human body, which normally has 3–7 degrees of freedom normally. The advantages of a robotic arm robot are more flexible movement and the ability to work in a limited space. Rotary arm and tracked transmission robots are two common types, and their printing range depends on the size of the robot arm. The rotary arm robot could rotate a level 360° from its fixed position; the tracked transmission robot can change position using a crawler drive. (3) With multiple degrees of freedom, a simple structure, and a fixed position, the cable-type automatic control robot has potential to position itself in a large space by adjusting and controlling the length of cable and the location of the end device. However, the accuracy needs further improvement.

Table 2. Summary of commonly used equipment 3D printing.

3D Printer System	Type	DOF	Features
Gantry system	Large dragon gate three-axis robot	3	Simple structure, high positioning accuracy, print range limited by a three-axis movement system
	Platform gantry three-axis robot		
Robotic arm	Rotary arm robot	3–7	Ability to work in limited space, high flexibility, higher accuracy
	Tracked transmission robot		
The cable type	Cable-type automatic control robot	N	Multiple degrees of freedom, poor positioning accuracy

3. Advantages of 3D Printing Technology in Pavement Maintenance

3.1. Traditional Repair Methods of Cracks and Potholes

According to ASTM D6433-07 (Standard Practice for Roads and Parking Lots Pavement Condition Index Surveys) [54], nineteen types of asphalt-surfaced distresses have been listed, including ride quality, alligator cracking (fatigue), bleeding, block cracking, bumps and sags, corrugation, depression, edge cracking, joint reflection cracking, lane/shoulder

drop-off, longitudinal and transverse cracking, patching and utility cut patching, potholes, polished aggregate, railroad crossing, rutting, shoving, slippage cracking, swell, weathering and raveling.

Cracking [55] is a typical distress of asphalt pavement, the common types, causes, description, and severity level of which are shown in Table 3. Cracking [56] will affect the driving stability of vehicles but also increase the impact load of the pavement. When water and other harmful substances enter the interior of the road through cracks, the stability of the pavement base and subgrade will be affected, and further bleeding, bumps and sags, etc. will be produced. Therefore, the quality, capacity, and service life of the road will be affected.

Common crack repair methods [57,58] include pouring, sealing, paving, pressure pouring, and digging-patching (in Figure 1a,b). Liquid modified asphalt and resin are commonly used to fill cracks directly, or seal bands made of fiber and modified asphalt are applied to seal cracks [59,60]. The advantages of pouring and sealing include easy construction, low technical difficulty, and low cost. The specific steps are to spray emulsified asphalt in the cracking area and then compact it with a roller after spreading stone crumbs or coarse sand. The shortcomings of the paving method are wasted materials and the complexity of the process. Pressure pouring is suitable for cracks in the internal structure of roads. First, surface cracks are sealed with resin, and then internal cracks are filled with cement paste with a slurry press through pre-buried pouring pipes. Pressure pouring requires a larger number of workers, greater costs, and greater internal structural stability of the road. For repaired cracks or cracks with serious deformation, the surrounding band needs to be excavated and backfilled with asphalt concrete for a more thorough repair of the cracks. For cracks with serious deformation or repaired cracks, the surrounding band needs to be excavated and backfilled with asphalt mixture for thorough repair.



Figure 1. Traditional repair methods of crack and pothole: (a) pouring cracking, (b) sealing cracking, (c) digging-patching of potholes. (@Tai'an City Fang Shuo Engineering Materials Co., Ltd.).

Table 3. Common types and severity level of cracking [54].

Type	Cause	Description	Level	Grading Basis
Longitudinal cracking	Poorly constructed paving lane joint, shrinkage of the AC surface, daily temperature cycling, reflective crack	Cracks parallel to the pavement's centerline or laydown direction	L	Nonfilled crack width < 10 mm, or filled crack of any width.
			M	Nonfilled crack width ≥ 10 mm and <75 mm, nonfilled crack ≤ 75 mm surrounded by light and random cracking; or filled crack is of any width surrounded by light random cracking
Transverse cracking	Structure of foundation and subgrade, not usually load associated	Cracks extend across the pavement at approximate right angles to the pavement centerline		
Joint reflection cracking	Cracks caused mainly by thermal or moisture-induced movement of the PCC slab beneath the AC surface	On asphalt-surfaced pavements be laid over a PCC slab, different from any other type of base (cement- or lime-stabilized)	H	Crack filled or nonfilled surrounded by medium- or high-severity cracking; nonfilled crack > 75 mm, or a crack of any width where approximately 100 mm of pavement around the crack is severely broken.
Alligator cracking (fatigue)	Interconnecting cracks caused by fatigue failure of the asphalt concrete surface under repeated traffic loading	Cracks connect, forming many sided, sharp-angled pieces, pieces generally less than 0.5 m on the longest side	L	Parallel longitudinal hairline cracks, a few interconnecting cracks, not spalled crack.
			M	Light alligator cracks into a pattern or network, lightly spalled.
			H	Pieces be defined and spalled at the edges well, some pieces may rock under traffic.
Block cracking	Interconnected cracks caused by shrinkage and daily temperature cycling, resulting in daily stress/strain cycling	Divide the pavement into approximately rectangular pieces, in size from approximately 0.3 by 0.3 m to 3 by 3 m	L	Blocks defined by low-severity cracks.
			M	Blocks defined by medium-severity cracks.
			H	Blocks defined by high-severity cracks.
Edge cracking	Cracks accelerated by traffic loading and frost-weakened base or subgrade near the edge of the pavement	Parallel, within 0.3 to 0.5 m of the outer edge of the pavement	L	Low or medium cracking with no breakup or raveling.
			M	Medium cracks with some breakup and raveling.
			H	Considerable breakup or raveling along the edge.
slippage cracking	Pavement surface slides or deforms due to braking or turning wheels	Crescent or half-moon shaped cracks, transverse to the direction of travel	L	Average crack width < 10 mm.
			M	Average crack width ≥ 10 and <40 mm, or crack area is moderately spalled, or surrounded by secondary cracks.
			H	Average crack width > 40 mm or the area around the crack is broken into easily removed pieces.

Note: For low-severity, medium-severity, and high-severity, see definitions of longitudinal transverse cracking.

Potholes [54] can affect pavement levelling and driving comfort. If potholes cannot be repaired in time, damage will develop faster under the combined effect of vehicle load and water, causing potential traffic safety risks. Common types and severity levels of potholes are shown in Table 4. Pothole repair methods can be divided into digging-patching, hot recycling, and jetting patching [61–63]. The main repair processes of digging-patching include removing old mixture from potholes, applying binder, paving, rolling, and compacting the new mixture. According to the mixing temperature of filled asphalt mixture, digging-patching (in Figure 1c) can be divided into hot patching using hot-mix asphalt mixture and cold patching using cold-mix asphalt mixture. The digging-patching method has a good repair effect although it is time consuming and requires various pieces of mechanical equipment. The hot recycling technique is based on the digging-patching approach and involves using the existing mixture. By filling the excavation site with a mixture of the existing mixture, regenerant material, and new mixture, it is possible to reduce waste and lower maintenance costs. However, the effectiveness of the repairs needs to be enhanced. The jetting patching method involves cleaning potholes with a high-strength air flow and then jetting aggregate and emulsified asphalt into the holes without compaction, which shortens the repair time. However, because the underlying issues at the bottom of the potholes cannot be completely removed, the repair life is short-lived.

Table 4. Common types and severity level of potholes [54].

Type	Cause	Description	Grading Basis of Severity Level		
			Maximum depth of pothole	Average diameter (mm)	
Potholes	Impact of traffic load, water-temperature cycle effect	Less than 750 mm in diameter bowl-shaped depressions in the pavement surface, sharp edges, vertical sides near the top of the hole.	100 to 200	200 to 450	450 to 750
			13 to \leq 25 mm	L	L
			>25 and \leq 50 mm	L	M
			>50 mm	M	H

3.2. Differences between 3D Printing Technology and Traditional Methods in Pavement Maintenance

Ultimately, 3D printing technology for repairing pavement distresses mainly includes the following steps. (1) Establishing a 3D digital model [64,65] of pavement distress. Common 3D modelling methods for pavement distress include photographic and laser scanning methods. Based on fast-developing pavement distress intelligent detection equipment, the photographic method could achieve accurate identification of pavement distress and acquisition of information about the distressed area. A 3D model could be built by identifying information from 2D images at different angles through vision technology. The laser scanning method is combined with a 3D optical system. By scanning the outer contour of the pavement distress, a series of point clouds and other data are obtained for reverse 3D modelling. (2) Three-dimensional model slicing and path planning [66–68]. Based on a combination of efficiency and accuracy, a 3D digital model of the distress area is sliced according to the selected thickness and direction to obtain information about the 2D print plane. If slicing direction and thickness are not selected properly, the accuracy of the repair will be affected. It is important to select the appropriate algorithm for 3D printing path planning so that the 2D plane contour could be filled by material scans along a reasonable path. (3) Three-dimensional printing repair [69]: selecting materials, type, and equipment of 3D printing to fill the pavement distress. The repair method can be divided into direct repair and indirect repair. Direct repair refers to in situ 3D printing. Material is filled into the distress by 3D printing, and the repair work is completed on site. Indirect repair refers to pre-fabricated repair pieces that correspond to the distress based on a 3D digital model.

(1) According to combining advanced technologies in the fields of mechanics, control, and computers, 3D printing technology [70] is greatly improving the automation of pavement distress maintenance and reducing the use of manpower. Therefore, the risk

of workers in places with heavy traffic can be reduced. In addition, the limitations of special climatic conditions and geographical locations on pavement maintenance can be decreased [71]. (2) Because of the standardization and precision of identification and filling of 3D printing maintenance [72], the excessive dependence on experience in traditional maintenance methods is avoided, and the problem of over- or under-filling of pavement distress in non-standardized construction is solved. (3) In the traditional maintenance of cracks and potholes, serious diseases are usually repaired thoroughly [73,74]. As a means of daily maintenance, 3D printing maintenance is mainly suitable for initial development of cracks and potholes. By promptly repairing and filling the initial distress of pavement, the development trend can be slowed down, the service time can be extended, and the service quality can be improved.

4. 3D Printing Technology in Pavement Maintenance

4.1. Asphalt as 3D Printing Material

As asphalt is a temperature-sensitive material with special mechanical properties, the viscoelastic properties of asphalt [61,75–77] can be changed with temperature variation. The stress-strain curves of asphalt are nonlinear under loading. In order to describe the mechanical properties of asphalt in the viscoelastic state more accurately, the stiffness modulus (ratio of stress to total strain under a certain time (t) and temperature (T)) [78,79] is commonly used. The stiffness modulus can describe the properties of asphalt, but it also contains the effects of temperature and load time. (1) The fluidity and plastic deformation capacity of asphalt would improve with the increase in temperature, accompanied by a decrease in stiffness modulus. The viscosity and deformation would enhance with the reduction of temperature. (2) With the shortening of the loading time, the stiffness modulus of asphalt increases and the deformation resistance becomes stronger.

Materials used for 3D printing require essential printability, including fluidity, extrudability, and buildability [71,80]. Fluidity refers to the ability of material to move smoothly during feeding and to provide a continuous material to print nozzles. Extrudability refers to the ability of material to extrude smoothly from the print nozzle without blockage or salivation. Buildability refers to the ability for material to resist its own gravity and that of subsequent print layers without deformation and to ensure good interlaminar bonding. At higher temperature, asphalt material has good fluidity and extrudability. At lower temperature, good bonding between layers can be ensured based on the greater viscosity of asphalt. The requirements of buildability can be met through deformation resistance. Therefore, the requirement of 3D printing can be fulfilled by controlling the temperature to regulate the printability of asphalt. In addition to common based and polymer modified asphalt, fine aggregate or fiber [81,82] can be added to expand the scope of application for 3D asphalt printing technology.

4.2. Types of 3D Asphalt Printing Technology

As summarized in Section 2.2., which covers the printing principle and typical materials used in different 3D printing technologies, the following insights can be gleaned. Out of the seven types of 3D printing technologies, the material used in vat photopolymerization is photosensitive. Binder jetting and sheet lamination, on the other hand, utilize powder and sheets as their respective materials. For powder bed fusion and directed energy deposition, metals and polymers would be melted by heat sources such as lasers and plasma arcs at above 3000 °C [83,84]. Due to the high cost and limited heating range, the above-mentioned five types of printing technologies are not suitable for use with asphalt.

Because the thermoplastic properties of asphalt fulfill the requirements for ME technology, it can be utilized for the 3D printing of asphalt. Materials with similar properties to asphalt such as PLA [85] and TPU [86] have been widely used in industrial manufacturing for production of handicrafts, models, etc. The printing parameters and path planning of material extrusion have been researched in depth. In the realm of construction engineering, 3D concrete printing has made significant strides in terms of efficiency and versatility

due to its ability to quickly form irregular structures. Screw extrusion [87] is the most commonly used method for feeding material in large-scale 3D concrete printing, thanks to its high efficiency, precise accuracy, straightforward design, and low cost. This makes screw extrusion an ideal choice for material extrusion in the 3D printing of asphalt.

Material jetting is the process of depositing ejected fluid materials layer by layer. Among materials commonly used in material jetting, photosensitive resin, concrete, and metal powders can be hardened by ultraviolet ray, hydration reaction, and low temperature, respectively [88]. Because asphalt hardens at a low temperature, material jetting can also be used for 3D asphalt printing. Different from filamentary asphalt extruded in material extrusion, droplet asphalt is jetted in material jetting technology at a higher printing temperature. Droplet asphalt is less controllable and less accurate than filamentary asphalt, so the application of material jetting should take full advantage of its high efficiency. Material jetting can be combined with air-feeding as a supplemental method of 3D asphalt printing.

4.3. Equipment of 3D Asphalt Printing Technology

In the existing research, some scholars have developed the equipment of 3D printing asphalt technology [89]. In 2018, based on the frame structure and control system of RepRap Mendel 90, Jackson et al. [90] modified the print head to 3D print granular asphalt at a printing temperature of 125–135 °C (in Figure 2a,b). The 3D printed asphalt showed up to nine times the ductility of cast samples with similar fracture strengths. A stepper motor was used to drive an auger screw. Asphalt was melted in a heating aluminum jacket by a thermistor, and a metal nozzle was used to improve heat conduction. Although the device achieved 3D asphalt printing, its print range was limited by the three-axis movement system, and it would be difficult for the print scale to meet the requirements of pavement maintenance, causing difficulties in practical engineering applications onsite. However, it can be used to make prefabricated patches in indirect repair. In 2018, researchers from Leeds University [91] equipped a six-rotor unmanned aerial vehicle (UAV) with a delta-style 3D printer (in Figure 2c). The UAV can fill potholes using a printer head after detecting them. The UAV improves the mobility of the asphalt printing device, but how it might carry enough asphalt for repair is a problem that needs to be solved.

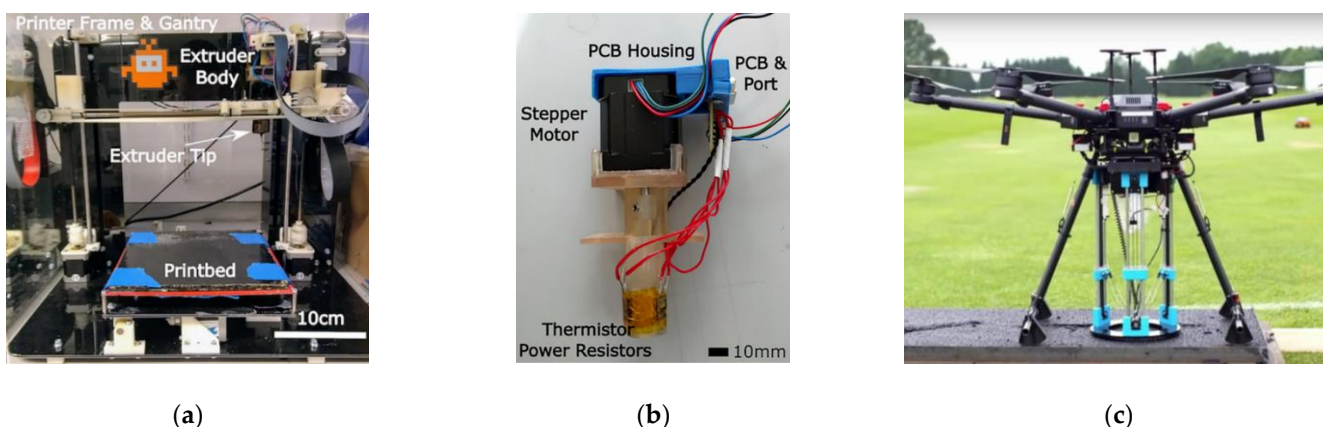


Figure 2. Equipment of 3D asphalt printing technology: (a) whole system of 3D asphalt printer, (b) complete extruder of 3D asphalt printer [90], (c) a six-rotor unmanned aerial vehicle (UAV) with a delta-style 3D printer [91].

Figure 3 shows a mobile 3D asphalt printing robot (hereafter referred to as “equipment”) from the Hebei University of Technology. The equipment mainly consists of a lithium battery crawler vehicle, a robotic arm, an image acquisition system of pavement distress, a screw feed component, and a control system. The crawler vehicle is used to carry other components and move flexibly during the maintenance of early cracks and light potholes in asphalt pavements. The robot arm base can rotate 360 degrees, and the large

arm and small arm can rotate 90 degrees and 180 degrees, respectively, ensuring flexible and accurate movement of the screw feed component at the end of the robot arm. The image acquisition system of pavement distress is used to collect information on early cracks and light potholes in pavement to provide a foundation for building 3D digital models, either with digital cameras or 3D laser scanners. The screw feed component is used to heat asphalt and extrude it precisely with 3D printing path planning and detection of the required amount. After the control system builds 3D digital models of the asphalt pavement distress using the image acquisition system, the results of slicing and path planning would be determined by the slicing software. Then, the movement of the robot arm is controlled to extrude fused asphalt from the extrusion nozzle to ensure the cooperative operation of equipment components in 3D printing maintenance of early cracks and light potholes.

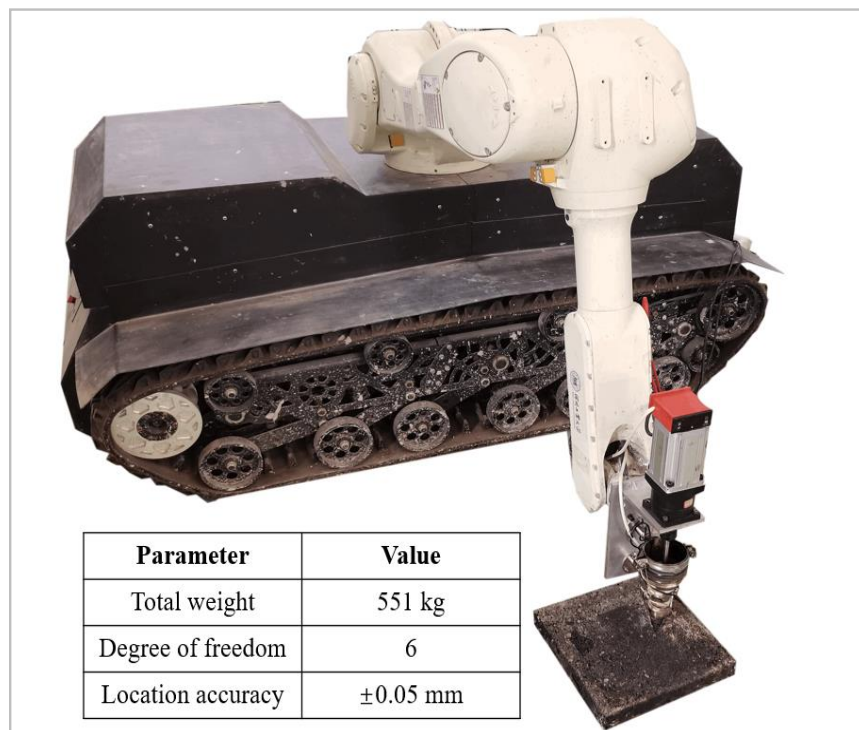


Figure 3. Mobile 3D asphalt printing robot (@HEBUT LAB).

Equipment with a good balance of accuracy and flexibility in terms of printing scale would meet the practical needs of engineering. Furthermore, it would have the capability to carry a sufficient amount of asphalt for maintenance. As a result, it could effectively adapt to the nature of asphalt pavement distress maintenance during extended construction at dispersed job sites.

5. Conclusions

The advancement of 3D printing technology in terms of precision, efficiency, and automation has been analyzed, with a focus on its potential to revolutionize traditional maintenance methods for asphalt pavement cracks and potholes. The benefits of 3D asphalt printing technology for pavement maintenance have been summarized, and its potential application in terms of materials, technology, and equipment has been evaluated. As a result, the following suggestions and conclusions are proposed.

- (1) The implementation of 3D printing technology in the maintenance engineering of cracks and shallow potholes has the potential to significantly improve automation, precision, and standardization in the field. This can result in a reduced risk for workers during construction, a decrease in environmental limitations, and an improvement in maintenance quality;

- (2) Asphalt, due to its favorable printability, can be utilized as a 3D printing material in combination with material extrusion and material jetting technologies for pavement maintenance;
- (3) A mobile 3D asphalt printing robot equipped with a screw extrusion device is the recommended primary equipment for 3D asphalt printing technology in pavement maintenance engineering on site, based on the requirements of printing scale, flexibility, and accuracy;
- (4) To minimize traffic control and increase maintenance efficiency, the use of UAVs equipped with air-feeding 3D printing equipment is suggested for the maintenance of both dense and light cracks, though further improvements in their range and load capacity are necessary.

Author Contributions: Conceptualization, F.G. and Z.Y.; resources, Q.W.; writing—original draft preparation, X.C. and F.G.; writing—review and editing, F.G. and X.C.; visualization, Y.C.; supervision, Z.Y.; funding acquisition, F.G. and Y.L. All authors have read and agreed to the published version of the manuscript.

Funding: This material is based in part upon work supported by the National Natural Science Foundation of China (52008154 and 51978074), the Hebei Science and Technology Department (E2021202074), and Special Funds for Jointly Building Colleges and Universities in Tianjin (280000-299).

Institutional Review Board Statement: Not applicable.

Informed Consent Statement: Not applicable.

Data Availability Statement: Not applicable.

Conflicts of Interest: The authors declare no conflict of interest.

References

1. Kogbara, R.B.; Masad, E.A.; Kassem, E.; Scarpas, A.; Anupam, K. A state-of-the-art review of parameters influencing measurement and modeling of skid resistance of asphalt pavements. *Constr. Build. Mater.* **2016**, *114*, 602–617. [[CrossRef](#)]
2. Cheng, C.; Cheng, G.; Gong, F.Y.; Fu, Y.R.; Qiao, J.G. Performance evaluation of asphalt mixture using polyethylene glycol polyacrylamide graft copolymer as solid-solid phase change materials. *Constr. Build. Mater.* **2021**, *300*, 124221. [[CrossRef](#)]
3. Cheng, C.; Gong, F.Y.; Fu, Y.R.; Liu, J.; Qiao, J.G. Effect of polyethylene glycol/polyacrylamide graft copolymerizaton phase change materials on the performance of asphalt mixture for road engineering. *J. Mater. Res. Technol.* **2021**, *15*, 1970–1983. [[CrossRef](#)]
4. Zakeri, H.; Moghadas Nejad, F.; Fahimifar, A. Image based techniques for crack detection, Classification and Quantification in Asphalt Pavement: A Review. *Arch. Comput. Methods Eng.* **2017**, *24*, 935–977. [[CrossRef](#)]
5. Wang, L.; Ren, M.D.; Xing, Y.M.; Chen, G. Study on affecting factors of interface crack for asphalt mixture based on microstructure. *Constr. Build. Mater.* **2017**, *156*, 1053–1062. [[CrossRef](#)]
6. Yi-Chang, T.; Vivek, K.; Russell, M.M. Critical assessment of pavement distress segmentation methods. *J. Transp. Eng.* **2010**, *136*, 11–19.
7. JTG. Ministry of Transport of the People's Republic of China. *Statistics Bulletin of Transportation Industry Development in 2021*; Ministry of Transport of the People's Republic of China: Beijing, China, 2021. (In Chinese)
8. Tan, Y.Q.; Guo, M.; Cao, L.P.; Zhang, L. Performance optimization of composite modified asphalt sealant based on rheological behavior. *Constr. Build. Mater.* **2013**, *47*, 799–805. [[CrossRef](#)]
9. Luo, X.; Gu, F.; Ling, M.; Lytton, R.L. Review of mechanistic-empirical modeling of top-down cracking in asphalt pavements. *Constr. Build. Mater.* **2018**, *191*, 1053–1070. [[CrossRef](#)]
10. Liu, M.; Han, S.; Shang, W.; Qi, X.; Dong, S.; Zhang, Z. New polyurethane modified coating for maintenance of asphalt pavement potholes in winter-rainy condition. *Prog. Org. Coat.* **2019**, *133*, 368–375. [[CrossRef](#)]
11. Wang, H. Approaches to safety management in daily maintenance of expressway. *Commun. Sci. Technol.* **2020**, *43*, 252–253. (In Chinese)
12. Jia, Y.S.; Wang, S.Q.; Huang, A.Q.; Gao, Y.; Wang, J.S.; Zhou, W. A comparative long-term effectiveness assessment of preventive maintenance treatments under various environmental conditions. *Constr. Build. Mater.* **2021**, *273*, 121717. [[CrossRef](#)]
13. The Third industrial revolution: The digitisation of manufacturing will transform the way goods are made-and change the politics of jobs too. *Economist* **2012**.
14. Aberoumand, M.; Soltanmohammadi, K.; Soleyman, E.; Rahmatabadi, D.; Ghasemi, I.; Baniassadi, M.; Abrinia, K.; Baghani, M. A comprehensive experimental investigation on 4D printing of PET-G under bending. *J. Mater. Res. Technol.* **2022**, *18*, 2552–2569. [[CrossRef](#)]

15. Ngo, T.D.; Kashani, A.; Imbalzano, G.; Nguyen, K.T.Q.; Hui, D. Additive manufacturing (3D printing): A review of materials, methods, applications and challenges. *Compos. Part B-Eng.* **2018**, *143*, 172–196. [[CrossRef](#)]
16. Rahmatabadi, D.; Soltanmohammadi, K.; Aberoumand, M.; Soleyman, E.; Ghasemi, I.; Baniassadi, M.; Abrinia, K.; Bodaghi, M.; Baghani, M. Development of Pure Poly Vinyl Chloride (PVC) with Excellent 3D Printability and Macro- and Micro-Structural Properties. *Macromol. Mater. Eng.* **2022**, *2200568*. [[CrossRef](#)]
17. Jaeheum, Y.; Julian, K.; Wei, Y. Spall damage repair using 3D printing technology. *Autom. Constr.* **2018**, *89*, 266–274.
18. Chen, F.; Song, C.H.; Yang, Y.Q.; Wei, H.M.; Zhou, H. Surface quality and mechanical properties of 316L stainless steel manufactured by powder feeding laser additive and milling subtractive hybrid manufacturing. *Laser Optoelectron. Prog.* **2021**, *1–13*. (In Chinese)
19. Gao, W.; Zhang, Y.B.; Devarajan, R.; Karthik, R.; Chen, Y.; Christopher, B.W.; Charlie, C.L.W.; Yung, C.S.; Zhang, S.; Pablo, D.Z. The status, challenges, and future of additive manufacturing in engineering. *Comput.-Aided Des.* **2015**, *69*, 65–89. [[CrossRef](#)]
20. ISO/ASTM 52900-2021; Standard Terminology for Additive Manufacturing—General Principles—Terminology. ISO: Geneva, Switzerland, 2021.
21. Zhang, J.; Xiao, P. 3D printing of photopolymers. *Polym. Chem.* **2018**, *9*, 1530–1540. [[CrossRef](#)]
22. Kitamori, H.; Sumida, I.; Tsujimoto, T.; Shimamoto, H.; Murakami, S.; Ohki, M. Evaluation of mouthpiece fixation devices for head and neck radiotherapy patients fabricated in PolyJet photopolymer by a 3D printer. *Phys. Med.-Eur. J. Med. Phys.* **2019**, *58*, 90–98. [[CrossRef](#)]
23. Pagac, M.; Hajný, J.; Ma, Q.P.; Jancar, L.; Jansa, J.; Stefk, P.; Mesicek, J. A review of vat photopolymerization technology: Materials, applications, challenges, and future trends of 3D printing. *Polymers* **2021**, *13*, 598. [[CrossRef](#)] [[PubMed](#)]
24. Shinde, V.V.; Celestine, A.D.; Beckingham, L.E.; Beckingham, B.S. Stereolithography 3D printing of microcapsule catalyst-based self-healing composites. *Acs Appl. Polym. Mater.* **2020**, *2*, 5048–5057. [[CrossRef](#)]
25. Mu, Q.Y.; Wang, L.; Dunn, C.K.; Kuang, X.; Duan, F.; Zhang, Z.; Qi, H.J.; Wang, T.J. Digital light processing 3D printing of conductive complex structures. *Addit. Manuf.* **2017**, *18*, 74–83. [[CrossRef](#)]
26. Tan, P.F.; Shen, F.; Tey, W.S.; Zhou, K. A numerical study on the packing quality of fibre/polymer composite powder for powder bed fusion additive manufacturing. *Virtual Phys. Prototyp.* **2021**, *16*, S1–S18. [[CrossRef](#)]
27. Nematollahi, M.; Saghaian, S.E.; Safaei, K.; Bayati, P.; Bassani, P.; Biffi, C.; Tuissi, A.; Karaca, H.; Elahinia, M. Building orientation-structure-property in laser powder bed fusion of NiTi shape memory alloy. *J. Alloy. Compd.* **2021**, *873*, 159791. [[CrossRef](#)]
28. Jinoop, A.N.; Paul, C.P.; Kumar, J.G.; Anilkumar, V.; Singh, R.; Rao, S.; Bindra, K.S. Influence of heat treatment on the microstructure evolution and elevated temperature mechanical properties of Hastelloy-X processed by laser directed energy deposition. *J. Alloys Compd.* **2021**, *868*, 159207. [[CrossRef](#)]
29. Kovalchuk, D.; Melnyk, V.; Melnyk, I.; Savvakin, D.; Dekhtyar, O.; Stasiuk, O.; Markovsky, P. Microstructure and properties of Ti-6Al-4V articles 3D-printed with co-axial electron beam and wire technology. *J. Mater. Eng. Perform.* **2021**, *30*, 5307–5322. [[CrossRef](#)]
30. Dalaei, M.; Cheaitani, F.; Arabi-Hashemi, A.; Rohrer, C.; Weisse, B.; Leinenbach, C.; Wegener, K. Feasibility study in combined direct metal deposition (DMD) and plasma transfer arc welding (PTA) additive manufacturing. *Int. J. Adv. Manuf. Technol.* **2020**, *106*, 4375–4389. [[CrossRef](#)]
31. Zhang, C.C.; Wei, H.L.; Liu, T.T.; Jiang, L.Y.; Yang, T.; Liao, W.H. Influences of residual stress and micro-deformation on microstructures and mechanical properties for Ti-6.5Al-3.5Mo-1.5Zr-0.3Si alloy produced by laser powder bed fusion. *J. Mater. Sci. Technol.* **2021**, *75*, 174–183. [[CrossRef](#)]
32. Phan, M.A.L.; Fraser, D.; Gulizia, S.; Chen, Z.W. Mechanism of hot crack propagation and prevention of crack formation during electron beam powder bed fusion of a difficult-to-weld Co-Cr-Ni-W superalloy. *J. Mater. Process. Technol.* **2021**, *293*, 117088. [[CrossRef](#)]
33. Ahn, D.G. Directed energy deposition (DED) process: State of the art. *Int. J. Precis. Eng. Manuf.-Green Technol.* **2021**, *8*, 703–742. [[CrossRef](#)]
34. Feenstra, D.R.; Banerjee, R.; Fraser, H.L.; Huang, A.e.; Molotnikov, A.; Birbilis, N. Critical review of the state of the art in multi-material fabrication via directed energy deposition. *Curr. Opin. Solid State Mater. Sci.* **2021**, *25*, 100924. [[CrossRef](#)]
35. Ziaee, M.; Crane, N.B. Binder jetting: A review of process, materials, and methods. *Addit. Manuf.* **2019**, *28*, 781–801. [[CrossRef](#)]
36. Oliveira, J.P.; LaLonde, A.D.; Ma, J. Processing parameters in laser powder bed fusion metal additive manufacturing. *Mater. Des.* **2020**, *193*, 108762. [[CrossRef](#)]
37. Tymrak, B.M.; Kreiger, M.; Pearce, J.M. Mechanical properties of components fabricated with open-source 3-D printers under realistic environmental conditions. *Mater. Des.* **2014**, *58*, 242–246. [[CrossRef](#)]
38. Wickramasinghe, S.; Do, T.; Tran, P. FDM-based 3D printing of polymer and associated composite: A review on mechanical properties, defects and treatments. *Polymers* **2020**, *12*, 1529. [[CrossRef](#)]
39. Dawoud, M.; Taha, I.; Ebeid, S.J. Mechanical behaviour of ABS: An experimental study using FDM and injection moulding techniques. *J. Manuf. Process.* **2016**, *21*, 39–45. [[CrossRef](#)]
40. Bardot, M.; Schulz, M.D. Biodegradable poly(Lactic Acid) nanocomposites for fused deposition modeling 3D printing. *Nanomaterials* **2020**, *10*, 2567. [[CrossRef](#)]
41. Wang, J.; Yang, B.; Lin, X.; Gao, L.; Liu, T.; Lu, Y.L.; Wang, R.G. Research of TPU materials for 3D printing aiming at non-pneumatic tires by FDM method. *Polymers* **2020**, *12*, 2492. [[CrossRef](#)]

42. Rahmatabadi, D.; Ghasemi, I.; Baniassadi, M.; Abrinia, K.; Baghani, M. 3D printing of PLA-TPU with different component ratios: Fracture toughness, mechanical properties, and morphology. *J. Mater. Res. Technol.* **2022**, *21*, 3970–3981. [CrossRef]
43. Moradi, M.; Aminzadeh, A.; Rahmatabadi, D.; Rasouli, S.A. Statistical and Experimental Analysis of Process Parameters of 3D Nylon Printed Parts by Fused Deposition Modeling: Response Surface Modeling and Optimization. *J. Mater. Eng. Perform.* **2021**, *30*, 5441–5454. [CrossRef]
44. Domenico, A.; Ferdinando, A.; Costantino, M.; Valentina, M. 3D printing of reinforced concrete elements: Technology and design approach. *Constr. Build. Mater.* **2018**, *165*, 218–231.
45. Nurhudan, A.I.; Supriadi, S.; Whulanza, Y.; Saragih, A.S. Additive manufacturing of metallic based on extrusion process: A review. *J. Manuf. Process.* **2021**, *66*, 228–237. [CrossRef]
46. Yu, T.Y.; Zhang, Z.Y.; Liu, Q.Y.; Kuliev, R.; Orlovskaya, N.; Wu, D.Z. Extrusion-based additive manufacturing of yttria-partially-stabilized zirconia ceramics. *Ceram. Int.* **2020**, *46*, 5020–5027. [CrossRef]
47. Azad, M.A.; Olawuni, D.; Kimbell, G.; Badruddoza, A.M.; Hossain, M.S.; Sultana, T. Polymers for extrusion-based 3D printing of pharmaceuticals: A holistic materials-process perspective. *Pharmaceutics* **2020**, *12*, 124. [CrossRef]
48. Wasti, S.; Adhikari, S. Use of Biomaterials for 3D printing by fused deposition modeling technique: A review. *Front. Chem.* **2020**, *8*, 315. [CrossRef] [PubMed]
49. Willems, E.; Turon-Vinas, M.; Camargo, D.S.B.; Van Hooreweder, B.; Zhang, F.; Van Meerbeek, B.; Vleugels, J. Additive manufacturing of zirconia ceramics by material jetting. *J. Eur. Ceram. Soc.* **2021**, *41*, 5292–5306. [CrossRef]
50. Yun, B.; Christopher, B.W. The effect of inkjetted nanoparticles on metal part properties in binder jetting additive manufacturing. *Nanotechnology* **2018**, *29*, 395706.
51. Bernhard, G.H.; Grohowski, J.A.; Schade, C.P.; Sheffield, P.; Crowder, S. Comparison of Ti-6Al-4V materials fabricated via mim and binder-jet printing. *Int. J. Powder Metall.* **2021**, *57*, 31–36.
52. Huang, S.J.; Ye, C.S.; Zhang, H.P.; Fan, Z.T. Additive manufacturing of thin alumina ceramic cores using binder-jetting. *Addit. Manuf.* **2019**, *29*, 100802. [CrossRef]
53. Viktor, M.; Venkatesh, N.N.; Frank, W.; Mathias, N.T.; Jens, O.; Martin, K. Large-scale digital concrete construction—CONPrint3D concept for on-site, monolithic 3D-printing. *Autom. Constr.* **2019**, *107*, 102933.
54. ASTM D6433-07; Standard Practice for Roads and Parking Lots Pavement Condition Index Surveys. ASTM: West Conshohocken, PA, USA, 2016.
55. Liu, J.W.; Yang, X.; Stephen, L.; Wang, X.; Luo, S.; Vincent, C.S.L.; Ding, L. Automated pavement crack detection and segmentation based on two-step convolutional neural network. *Comput.-Aided Civ. Infrastruct. Eng.* **2020**, *35*, 1291–1305. [CrossRef]
56. Wu, S.Y.; Liu, Q.; Yang, J.; Yang, R.C.; Zhu, J.P. Study of adhesion between crack sealant and pavement combining surface free energy measurement with molecular dynamics simulation. *Constr. Build. Mater.* **2020**, *240*, 117900. [CrossRef]
57. JTG 5210-2018; Highway Performance Assessment Standards. Ministry of Transport of the People's Republic of China: Beijing, China, 2018. (In Chinese)
58. Ma, D.C.; Yang, S. Applicability and economic analysis of asphalt road crack and pothole technique. *Constr. Mach.* **2007**, *17*, 82–85. (In Chinese)
59. Gong, F.Y.; Liu, Y.; You, Z.P.; Zhou, X.D. Characterization and evaluation of morphological features for aggregate in asphalt mixture: A review. *Constr. Build. Mater.* **2021**, *273*, 121989. [CrossRef]
60. Kim, S.J.; Ko, K.J. Asphalt sealant containing the waste lubricant oil. *Elastomers Compos.* **2009**, *44*, 69–75.
61. Li, X.L.; Zhou, Z.H.; Ye, J.H.; Zhang, X.A.; Wang, S.Y.; Diab, A. High-temperature creep and low-temperature relaxation of recycled asphalt mixtures: Evaluation and balanced mix design. *Constr. Build. Mater.* **2021**, *310*, 125222. [CrossRef]
62. Byzyka, J.; Rahman, M.; Chamberlain, D.A. Thermal analysis of hot mix asphalt pothole repair by finite-element method. *J. Transp. Eng. Part B-Pavements* **2020**, *146*, 04020029. [CrossRef]
63. Geng, L.T.; Xu, Q.; Yu, X.X.; Jiang, C.L.; Zhang, Z.; Li, C.Z. Laboratory performance evaluation of a cold patching asphalt material containing cooking waste oil. *Constr. Build. Mater.* **2020**, *246*, 117637. [CrossRef]
64. Li, B.; Meng, L.F.; Wang, H.Y.; Li, J.; Liu, C.M. Rapid prototyping eddy current sensors using 3D printing. *Rapid Prototyp. J.* **2018**, *24*, 106–113. [CrossRef]
65. Liang, Y.Y.; Zhao, J.; Huang, Q.L.; Hu, P.; Xiao, C.F. PVDF fiber membrane with ordered porous structure via 3D printing near field electrospinning. *J. Membr. Sci.* **2021**, *618*, 118709. [CrossRef]
66. McLouth, T.D.; Severino, J.V.; Adams, P.M.; Patel, D.N.; Zaldivar, R.J. The impact of print orientation and raster pattern on fracture toughness in additively manufactured ABS. *Addit. Manuf.* **2017**, *18*, 103–109. [CrossRef]
67. Huang, Y.M.; Jiang, C.P. Curl distortion analysis during photopolymerisation of stereolithography using dynamic finite element method. *Int. J. Adv. Manuf. Technol.* **2003**, *21*, 586–595. [CrossRef]
68. Lin, S.; Xia, L.W.; Ma, G.W.; Zhou, S.W.; Xie, Y.M. A maze-like path generation scheme for fused deposition modeling. *Int. J. Adv. Manuf. Technol.* **2019**, *104*, 1509–1519. [CrossRef]
69. Li, J.Y.; He, F.; Shi, H.L.; Qin, K.Q. Application of 3D Printing Technology in Pavement Repair Engineering. *Highway* **2019**, *64*, 51–55. (In Chinese)
70. Tay, Y.W.D.; Panda, B.; Paul, S.C.; Mohamed, N.A.N.; Tan, M.J.; Leong, K.F. 3D printing trends in building and construction industry: A review. *Virtual Phys. Prototyp.* **2017**, *12*, 261–276. [CrossRef]

71. Gong, F.Y.; Cheng, X.J.; Chen, Y.; Liu, Y.; You, Z.P. 3D printed rubber modified asphalt as sustainable material in pavement maintenance. *Constr. Build. Mater.* **2022**, *354*, 129160. [[CrossRef](#)]
72. Luo, W.J.; Mao, Z.C.; Lu, H.Z.; Yang, J.; Ma, X.C.; Xu, L.J. Subversion of conventional construction: Building 3D printing technology. *IOP Conf. Ser. Earth Environ. Sci.* **2020**, *531*, 012005. [[CrossRef](#)]
73. Hao, Y.S.; Liu, X.D. Causes and treatment of asphalt pavement potholes on highways. *J. China Foreign Highw.* **2012**, *32*, 118–120. (In Chinese)
74. Han, C.Y.; Yuan, Y.S. Research on rapid repair technique of asphalt pavement pothole. *J. China Foreign Highw.* **2013**, *33*, 59–63. (In Chinese)
75. Zhu, J.Q.; Bj, R.B.; Niki, K. Polymer modification of bitumen: Advances and challenges. *Eur. Polym. J.* **2014**, *54*, 18–38. [[CrossRef](#)]
76. Polacco, G.; Filippi, S.; Merusi, F.; Stastna, G. A review of the fundamentals of polymer-modified asphalts: Asphalt/polymer interactions and principles of compatibility. *Adv. Colloid Interface Sci.* **2015**, *224*, 72–112. [[CrossRef](#)]
77. Gong, F.Y.; Guo, S.C.; Chen, S.Y.; You, Z.P.; Liu, Y.; Dai, Q.L. Strength and durability of dry-processed stone matrix asphalt containing cement pre-coated scrap tire rubber particles. *Constr. Build. Mater.* **2019**, *214*, 475–483. [[CrossRef](#)]
78. Capitao, S.D.; Picado-Santos, L.G.; Martinho, F. Pavement engineering materials: Review on the use of warm-mix asphalt. *Constr. Build. Mater.* **2012**, *36*, 1016–1024. [[CrossRef](#)]
79. Meneses, J.P.C.; Vasconcelos, K.; Bernucci, L.L.B. Stiffness assessment of cold recycled asphalt mixtures—Aspects related to filler type, stress state, viscoelasticity, and suction. *Constr. Build. Mater.* **2022**, *318*, 126003. [[CrossRef](#)]
80. Ma, G.W.; Wang, L.; Ju, Y. State-of-the-art of 3D printing technology of cementitious material—An emerging technique for construction. *Sci. China Technol. Sci.* **2018**, *61*, 475–495. [[CrossRef](#)]
81. Safi, B.; Saidi, M.; Daoui, A.; Bellal, A.; Mechkak, A.; Toumi, K. The use of seashells as a fine aggregate (by sand substitution) in self-compacting mortar (SCM). *Constr. Build. Mater.* **2015**, *78*, 430–438. [[CrossRef](#)]
82. Kurup, A.R.; Kumar, K.S. Effect of recycled PVC fibers from electronic waste and silica powder on shear strength of concrete. *J. Hazard. Toxic Radioact. Waste* **2017**, *21*, 06017001. [[CrossRef](#)]
83. Sing, S.L.; An, J.; Yeong, W.Y.; Wiria, F.E. Laser and electron-beam powder-bed additive manufacturing of metallic implants: A review on processes, materials and designs. *J. Orthop. Res.* **2016**, *34*, 369–385. [[CrossRef](#)]
84. DebRoy, T.; Wei, H.L.; Zuback, J.S.; Mukherjee, T.; Elmer, J.W.; Milewski, J.O.; Beese, A.M.; Wilson-Heid, A.; De, A.; Zhang, W. Additive manufacturing of metallic components—Process, structure and properties. *Prog. Mater. Sci.* **2018**, *92*, 112–224. [[CrossRef](#)]
85. Chacon, J.M.; Caminero, M.A.; Garcia-Plaza, E.; Nunez, P.J. Additive manufacturing of PLA structures using fused deposition modelling: Effect of process parameters on mechanical properties and their optimal selection. *Mater. Des.* **2017**, *124*, 143–157. [[CrossRef](#)]
86. Cong, L.; Yang, F.; Guo, G.H.; Ren, M.D.; Shi, J.C.; Tan, L. The use of polyurethane for asphalt pavement engineering applications: A state-of-the-art review. *Constr. Build. Mater.* **2019**, *225*, 1012–1025. [[CrossRef](#)]
87. Jacques, K.; Stephan, Z.; Gideon, V.Z. 3D concrete printing: A lower bound analytical model for buildability performance quantification. *Autom. Constr.* **2019**, *106*, 102904.
88. Lv, X.Y.; Ye, F.; Cheng, L.F.; Fan, S.W.; Liu, Y.S. Binder jetting of ceramics: Powders, binders, printing parameters, equipment, and post-treatment. *Ceram. Int.* **2019**, *45*, 12609–12624. [[CrossRef](#)]
89. Gong, F.Y.; Cheng, X.J.; Fang, B.J.; Cheng, C.; Liu, Y.; You, Z.P. Prospect of 3D printing technologies in maintenance of asphalt pavement cracks and potholes. *J. Clean. Prod.* **2023**, *397*, 136551. [[CrossRef](#)]
90. Richard, J.J.; Adam, W.; Mark, M. 3D printing of asphalt and its effect on mechanical properties. *Mater. Des.* **2018**, *160*, 468–474.
91. Fabbaloo. Available online: <https://www.fabbaloo.com/2018/07/repairing-potholes-with-3d-printers> (accessed on 12 February 2023).

Disclaimer/Publisher’s Note: The statements, opinions and data contained in all publications are solely those of the individual author(s) and contributor(s) and not of MDPI and/or the editor(s). MDPI and/or the editor(s) disclaim responsibility for any injury to people or property resulting from any ideas, methods, instructions or products referred to in the content.